

Measurement of F_2 and F_L at low Q^2 in ep interactions at HERA

T. Laštovička^{1,2}, on behalf of the H1 and Zeus Collaborations

¹ DESY Zeuthen, Platanenallee 6, D15738 Zeuthen, Germany, e-mail: lastovic@ifh.de

² Charles University, Faculty of Mathematics and Physics, V Holešovičkách 2, 18000 Prague 8, Czech Republic

Received: 15 November 2003 / Accepted: 7 January 2004 /

Published Online: 11 February 2004 – © Springer-Verlag / Società Italiana di Fisica 2004

Abstract. Preliminary data are presented on the proton structure functions F_2 and F_L measured in deep inelastic scattering in the kinematic region of low Bjorken x and low four-momentum transfer squared Q^2 by the H1 and ZEUS experiments.

1 Introduction

In the single-photon exchange approximation the reduced neutral current inclusive DIS cross section at low Q^2 is given as

$$\frac{Q^4 x}{2\pi\alpha^2 Y_+} \cdot \frac{d^2\sigma}{dx dQ^2} = \sigma_r = F_2(x, Q^2) - \frac{y^2}{Y_+} \cdot F_L(x, Q^2), \quad (1)$$

where $Y_+ = 1 + (1 - y)^2$. The inelasticity y is related to x and Q^2 as $y = Q^2/sx$, where s is the center of mass energy squared. The influence of the longitudinal structure function F_L on the reduced cross section σ_r is strongly suppressed for $y < 0.6$ due to the kinematic factor y^2/Y_+ and since $F_L \leq F_2$. Thus the measurement of σ_r at low y directly determines F_2 with a small correction for F_L , while F_L can be extracted at high y , resp. small x .

In the Quark Parton Model [1] the photon interacts with a spin 1/2 particle having only longitudinal momentum, which leads to [2] $F_L(x) = 0$. In Quantum Chromodynamics (QCD) quarks interact through gluons, which can split into quark anti-quark or gluon pairs. This way, the quark struck by a virtual photon has transverse momentum $\sim Q$, which leads to $F_L(x, Q^2) > 0$. Thus F_L is directly connected with the gluon distribution in the proton and can provide a sensitive test of perturbative QCD.

The analyses presented in this contribution were recently performed by the H1 and ZEUS collaborations. Details can be found in the quoted references while this summary is focused on the results.

2 Cross section measurements

The inclusive deep inelastic scattering cross section was measured at H1 during two dedicated running periods, denoted as *mb99* [3] and *svtx00* [4]. In both of them the H1 trigger system was set up to deliver minimum-biased

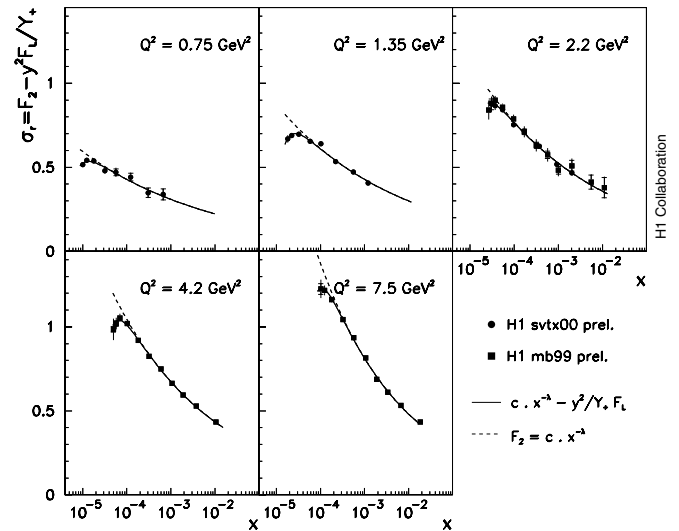


Fig. 1. The reduced cross section as a function of x in bins of Q^2 . Preliminary data by the H1 collaboration are shown. The inner error bars represent the statistical errors. The full errors include the statistical and systematic errors added in quadrature. The dashed lines show a function of the form $c \cdot x^{-\lambda}$ representing the F_2 contribution to the fitted cross section. The solid lines show fits of the form $\sigma_r = c \cdot x^{-\lambda} - y^2/Y_+ F_L$, from which F_L is extracted in the shape method, see text

inclusive low Q^2 data. Furthermore, in the *svtx00* sample the interaction vertex was shifted along the proton beam by about 70 cm in order to access the transition region from the non-perturbative to the deep-inelastic domain at even lower Q^2 . Figure 1 shows the measured cross section as a function of x in bins of Q^2 . With increase in statistics and new instrumentation the accuracy of the measurement is improved as compared to the previous low Q^2 data [5, 6]. The data were further used for various phenomenological studies, e.g. to study the rise of F_2 at low x .

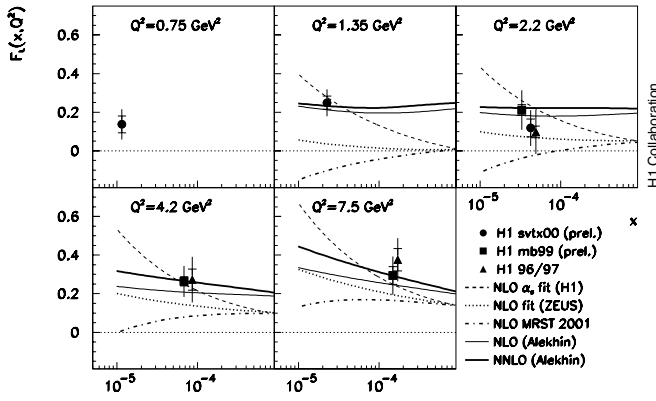


Fig. 2. Determination of $F_L(x, Q^2)$ (closed squares and circles) by the H1 collaboration from low Q^2 cross section measurements. The inner error bars correspond to statistical errors. The full errors include the statistical, uncorrelated and correlated systematic errors added in quadrature. The result is compared to various NLO and NNLO QCD fits and to the previous H1 determination [5] (triangles)

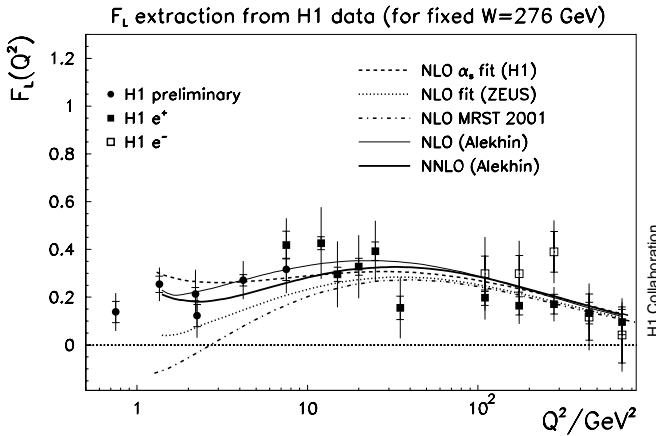


Fig. 3. Q^2 dependence of $F_L(x, Q^2)$ (at fixed $W = 276$ GeV), summarizing the data from the H1 experiment. The inner error bars represent the statistical errors. The full errors include the statistical, uncorrelated and correlated systematic errors added in quadrature. The result is compared to various NLO and NNLO QCD fits

3 F_L at very low Q^2

The new low Q^2 data, introduced in the previous section, were used to determine F_L . For fixed Q^2 , the inclusive cross section rises with decreasing x (see Fig. 1). However, at very low x (high y) a characteristic bending of the cross section can be noticed. This occurs at all Q^2 values at fixed $y \sim 0.5$ and is attributed to the contribution from the longitudinal structure function $F_L(x, Q^2)$. The shape of the cross section bending is driven by the kinematic factor y^2/Y_+ rather than by the behaviour of F_L . This observation is employed in the new method of F_L extraction at low Q^2 by the H1 collaboration [7].

The obtained F_L data are shown in Fig. 2 together with predictions of various higher order QCD fits, partially extrapolated below their minimum Q^2 of applica-

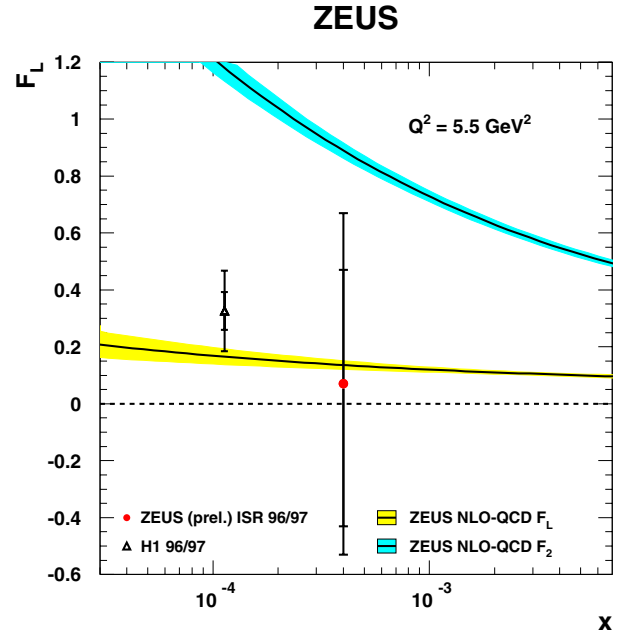


Fig. 4. A measurement of F_L by the ZEUS collaboration from the ISR analysis in a bin of $Q^2 = 5.5$ GeV². The result (closed circle) is compared to the previous H1 determination [5] (open triangle) and to F_L (lower band) and F_2 (upper band) from the ZEUS QCD fit [10]

bility. The values of $F_L(x, Q^2)$ are consistent with the previous determination by the H1 Collaboration (closed triangles), but are more precise and extend the kinematical region, in which $F_L(x, Q^2)$ is determined, to lower Q^2 . As can be seen from the different curves there is a significant uncertainty for the F_L prediction in the NLO QCD fits. This reflects the uncertainty of the initial gluon distribution. The H1 data clearly favor a positive, not small F_L at low Q^2 and small x , as is preferred by the H1 and Alekhin's fits while the MRST and ZEUS predictions are low. A negative F_L value at small x is experimentally ruled out by the measured turn-over of the reduced cross section, see Fig. 1, which leads to $F_L > 0$. It becomes evident from Fig. 2 that the x dependence of F_L needs to be measured which requires to operate HERA at reduced proton beam energy.

An overview of all current H1 data on $F_L(x, Q^2)$, from $Q^2 = 0.75$ GeV² to 700 GeV² and for fixed $W = 276$ GeV, is given in Fig. 3. It comprises the preliminary results of the low Q^2 analysis, the results based on data collected in 96/97 [5] and also the recently published high Q^2 results from e^+p and e^-p data [8]. All QCD fits describe the data at larger Q^2 while at lower Q^2 similar conclusions can be drawn as for the x dependence discussed above.

4 Initial state radiation analysis

In initial state radiation events (ISR) the lepton beam energy is varied due to a hard initial state photon emission. In [9] this class of events was used by ZEUS to measure the structure function F_2 in the kinematic range

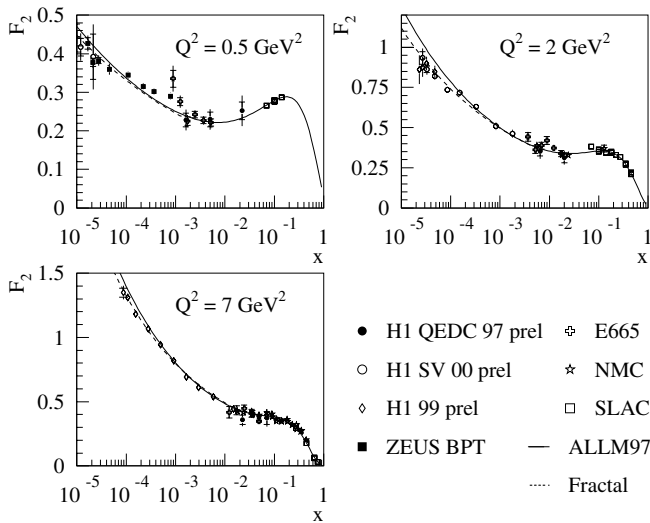


Fig. 5. Results of the F_2 measurement from QED Compton scattering (*closed circles*) compared with other measurements at HERA and fixed target experiments. The *solid line* depicts the ALLM97 parametrisation [12], while the *dashed line* represents the Fractal parametrisation [13], which is plotted in the range $y > 0.003$

$0.3 < Q^2 < 22 \text{ GeV}^2$ and $8 \times 10^{-6} < x < 1.8 \times 10^{-1}$ which was found to be consistent with previous measurements. Furthermore, the beam energy variation was employed to directly extract the longitudinal structure function F_L assuming F_2 to be well known in this kinematical region. The technique of this measurement is in detail described in [9]. The result is shown in Fig. 4, and it is compared to the previous H1 determination [5] and to ZEUS QCD fit [10] structure functions F_2 and F_L .

5 QED compton analysis

The proton structure function F_2 was measured in QED Compton scattering using data collected in 1997 by the H1 experiment [11]. The region of very low Q^2 , down to 0.1 GeV^2 , is accessed at medium Bjorken x . Hence, the measurement is complementary to the inclusive cross section measurements presented in Section 2. The results are in agreement with measurements from fixed target experiments in the region of overlap, see Fig. 5.

References

1. J.D. Bjorken: Phys. Rev. **179**, 1547 (1969)
2. C.G. Callan and D.J. Gross: Phys. Rev. Lett. **22**, 156 (1969)
3. H1: contributed paper **799** to EPS 2001, Budapest
4. H1: contributed paper **979** to ICHEP 2002, Amsterdam
5. H1: Eur. Phys. J. C **21**, 33-61 (2001)
6. H1: C. Adloff et al.: Nucl. Phys. B **497**, 3 (1997)
7. E. Lobodzinska: in "DIS 2003 - 11th Int. Workshop on Deep Inelastic Scattering", to be published
8. H1: Eur. Phys. J. C **30**, 1-32 (2003)
9. J. Cole: in "DIS 2003 - 11th Int. Workshop on Deep Inelastic Scattering", to be published
10. ZEUS: Phys. Rev. D **67**, 012007 (2003)
11. V. Lenderman: in "DIS 2003 - 11th Int. Workshop on Deep Inelastic Scattering", to be published
12. H. Abramowicz and A. Levy: hep-ph/9712415
13. T. Laštovička: Eur. Phys. J. C **24**, 529 (2002)